



# Integration of 2D and 3D Electrical Resistivity Tomography for Volumetric Investigation of Geologic Formations in a Sedimentary Terrain

Murphy Ogiemwonyi Iduseri<sup>1</sup>, Osisanya Olajuwon Wasii<sup>1\*</sup>, Avwenaghegha O. Jude<sup>2</sup>, Korode Akinjide Isaac<sup>3</sup>, Amoyedo Abiodun Adekunle<sup>3</sup>

<sup>1</sup>Department of Physics, University of Benin, Benin City, Nigeria

<sup>2</sup>Delta State University of Science and Technology Ozoro, Nigeria

<sup>3</sup>Department of Petroleum Engineering and Geosciences, Petroleum Training Institute, Effurun, Nigeria

## INFORMATION

### Article history

Received 13 February 2023

Revised 05 April 2023

Accepted 06 April 2023

### Keywords

Geologic formations

Electrical resistivity imaging

Volumetric estimation

Sedimentary terrain

Southern Nigeria

### Contact

\*Osisanya Olajuwon Wasii

[wasiu.osisanya@uniben.edu](mailto:wasiu.osisanya@uniben.edu)

## ABSTRACT

In a wide variety of research fields, including agriculture, botany, road construction and mineral exploration, it is crucial to analyse the volume of dominant geologic formations in an area especially those of very high economic importance. Volumetric evaluation of geologic formations is an essential stride towards economic and local content development. Ten (10) 2D geoelectrical resistivity profiles were gathered in parallel and perpendicular equidistant lines using the Wenner array with maximum electrodes spread of 200m to investigate the subsurface geological stratification in both the vertical and horizontal direction at Obaretin community in the Edo State, Nigeria. Using Earth Imager 2D software, 2D resistivity-depth models were created from the 2D resistivity dataset with the use of Wenner array. In order to create a 3D depth slice and a 3D block model for the subsurface stratification, the survey dataset was compiled into a single 3D data set and inverted using Res3Dinv software and Voxler 4.0 programs. The 2D resistivity imaging results revealed three geo-electric major layers at Obaretin, which are indicative of topsoil, silt sand, clayey sand, and lateritic sand with sandstone intercalations as the dominant geologic formations in the study area. The Resistivity lithology of the study area also showed three geo-electric subsurface layers to an appreciable depth of 40 m for Silt sand, topsoil (299–1791  $\Omega\text{m}$ ), lateritic sand with sandstones intercalations (985–3253  $\Omega\text{m}$ ), and clayey sand (48.9–1791  $\Omega\text{m}$ ) were delineated. The study revealed that the dominant formations are laterite, silt sand and clayey sand which showed an estimated volumetrics of 373,508m<sup>3</sup>, 520,320 m<sup>3</sup> and 194,800 m<sup>3</sup> per two million m<sup>3</sup> respectively which are in high economic quantities. Hence, the adoption of 2D and 3D electrical resistivity imaging has aided the successful volumetric assessment of geologic formations which are of high economic value in the study area.

## 1. Introduction

Geologic formations in the earth crust as natural resources have contributed tremendously to national development in many countries towards infrastructural development as aid to growth and progress in many areas as agriculture, botany, road construction and monitoring, pollution of contaminants to mention a few (Loke, 2000; Revil et al., 2005; Dahlin and Zhou, 2006; Panek et al., 2008; Schrott and Saas, 2008; Bery

et al., 2012; Loke, 2012; Bhattacharya and Shalivahan, 2016). Assessment of these formations is very paramount to harness their potential resources maximally. Geophysical exploration as well as other viable methods can serve as tools for investigating the presence or absence of mineralization in an area. Taking cognisance of geophysical investigation as an exploratory tool, Osisanya et al. (2017; 2020) mapped laterite deposits and clay deposits in the study area respectively using



2D resistivity imaging technique. It was observed that laterite deposits almost occur at the same depth within the subsurface and were in commercial quantity, while clay formations were sparsely deposited, thus, making them insufficient for commercial exploitation.

These results were validated with result of borehole log conducted in the area (Alile et al., 2011) which also revealed that the geologic formation sequence in the area is made up of lateritic soil, sand, clay, coarse sand, lignite, coarse gravel and sandstone. In another study by Aboralin et al. (2020) a multitechnique methodology was employed for mineral deposit exploration in a part of Igarra North Basement complex, Southwestern Nigeria. 2D Resistivity inversion showed anomalous zones with relatively low and high resistivity variation compared with the background trend which was interpreted as due to presence metallic sulphide/oxide deposit.

Electrical resistivity tomography (ERT) seems to be the most reliable method for imaging various types of deposits within the subsurface with high precision for near surface investigation (Piegari et al., 2009). In mineral exploration as well as geologic formation delineation, the ERT method has been used severally to map geologic boundary and mineral deposits both in massive form as well as pocket/disseminated deposits found close to the surface. It was stated that some complication might be experienced from interpreting void filled clay deposit or some bedrock that are rich in clay might be depicted with low resistivity values due to its capacity to retain large volume of water and grain boundaries with high conductivity (Robert et al., 2011; Xu et al., 2016; Bermejo et al., 2017; McCormack et al., 2017; Keshavarzi et al., 2017; Cheng et al., 2019). In northern Sardinia, bentonitic clay deposits were mapped using ERT which helped to define the extent and geometry of the deposits with high resolution (Longo et al., 2014).

## 2. The Basic Concept of 2D and 3D ERT Method

Electrical resistivity technique generates 2D and 3D resistivity models of the subsurface formation via electrodes measurement at the surface of the ground. The geologic formation delineation of electrical resistivity imaging is dependent on the lithological characteristics (e.g pure size dispersion, rate of water saturation and composition of pore water (Lesmes and Friedman, 2005; Cheng et al., 2019).

Primarily, the one-dimensional (1D) electrical method primarily known as vertical electrical sounding depends on the conception of horizontal layered earth model or homogeneous/isotropic earth layers, without taking lateral resistivity variation into consideration. The 2-D ERT technique provides the image of both lateral and vertical variation in ground resistivity measured using electrodes placed on the surface of the earth (Loke et al., 2013). The 2D resistivity model from a 2D ERT dataset provides a better approximation of the subsurface model of the earth (Eze et al., 2021).

Nevertheless, images resulting from 2D electrical resistivity surveys often produce misleading subsurface features, due to out-of-plane variation in apparent resistivity anomaly in

magnitude and location (Ahzegbobor et al., 2010 as cited in Eze et al., 2021). These errors usually arise because the underlying assumption of two dimensions for geological features is only an approximation; in reality, geological features/structures encountered in environmental/near surface investigations are intrinsically three dimensional (3D) in nature. Therefore, 3D models of the subsurface gives a more robust and precise result. ERT is mostly used to depict the inversion process along side with the imaging result. The electrical resistivity technique utilizes horizontal profiling and vertical (depth) sounding to generate a 2D or 3D of the subsurface image (Khalil et al., 2013).

For several years till now, Electrical Resistivity Imaging has been adopted in conducting environmental investigation, geotechnical survey, foundation studies, mineral deposit delineation, mining and groundwater investigation. Bery et al. (2012) conducted high resolution resistivity imaging and induced polarisation (IP) surveys over an area in Pagoh, Malaysia, and successfully delineated the iron ore body at the exploration stage.

Alile and Abraham (2015) collated 2D apparent resistivity data acquired in Benin City, Edo State, into 3D dataset and subsequently applied 3D resistivity inversion to invert the dataset. Their result demonstrated the effectiveness and resolution of the 3D resistivity tomography. Several researchers have applied 2D and 3D electrical resistivity imaging to solving many environmental and geological problems; Ahzegbobor et al., (2010) carried out an investigation in a crystalline basement complex in southwestern Nigeria with the aim of assessing the rate of fracturing and weathering of the subsurface formation in the study area, to determine its groundwater potential as well as investigate its competency for engineering purpose.

Eze et al. (2021) in their study on 'Numerical modeling of 2-D and 3-D geoelectrical resistivity data for engineering site investigation and groundwater flow direction study in a sedimentary terrain' detailed the theoretical concept and procedure for executing 2D and 3D resistivity modeling. The study validated the superiority of 3-D ERT to 2-D ERT in resolving complex heterogenous geological environment.

To determine the volumetrics of a suspected dominant occurrence of mineral using the 3D horizontal depth slice, a visual observation was used to estimate the area of zones measured through x-y axes from the 3D horizontal slices. A simple mathematical modeling approach was then used for the evaluation of the Sand volume. The estimate of identified sand area ( $\Delta A$ ) from a 3D horizontal slice was multiplied by the corresponding depth ( $\Delta Z$ ). The product is expressed as volume ( $\Delta V$ ) for the associated sand in a layer.

$$\Delta V = \Delta A \times \Delta Z \text{ (Abdullahi et al., 2013)} \quad (1)$$

The study area, Obaretin is an area with sparse or no subsurface information for volumetric assessment of geologic formation using 3D electrical resistivity imaging. This necessitated the use of high-resolution 3D electrical resistivity survey in delineating the subsoil strata in Obaretin communities, Edo State, Nigeria.

### 3. Local Geology of the Study Area

The study area Obaretin lies between Latitudes 6°2'30" to 6°12'30"N and Longitudes 5°32'30" to 5°45'0"N (Fig. 1). It has a minimum elevation of 25 m and maximum elevation of 52.3 m above sea level. The areas occupy the Southern part of Edo State which is a sedimentary terrain and is underlain by sedimentary rocks of Paleocene to Recent in age. The sedimentary rock contains about 90% of sand stone and shale intercalations (Alile et al., 2011). Edo State is situated in South southern part of Nigeria. The geological setting consists of the coastal plain sands often referred to as Benin sands of the Benin Formation. The Benin sands are partly marine, partly deltaic and partly lagoonal (Ogunsanwo,

1989), all indications of a shallow water environment of deposition. The formation is made up of top reddish clayey sand capping highly porous fresh water bearing loose pebbly sands, and sandstone with local thin clays and shale interbeds which are considered to be of braided stream origin. The formation is covered with loose brownish sand (quaternary drift) varying in thickness and is about 800 m thick; almost all of which is water bearing with water level varying from about 20 m to 52 m (Kogbe, 1989). The coastal plain sands in the study area is bounded by Alluvium and Mangrove swamps before it, and afterward it by the Bende Ameki Formation and Imo clay-shale group (Alile and Abraham, 2015).

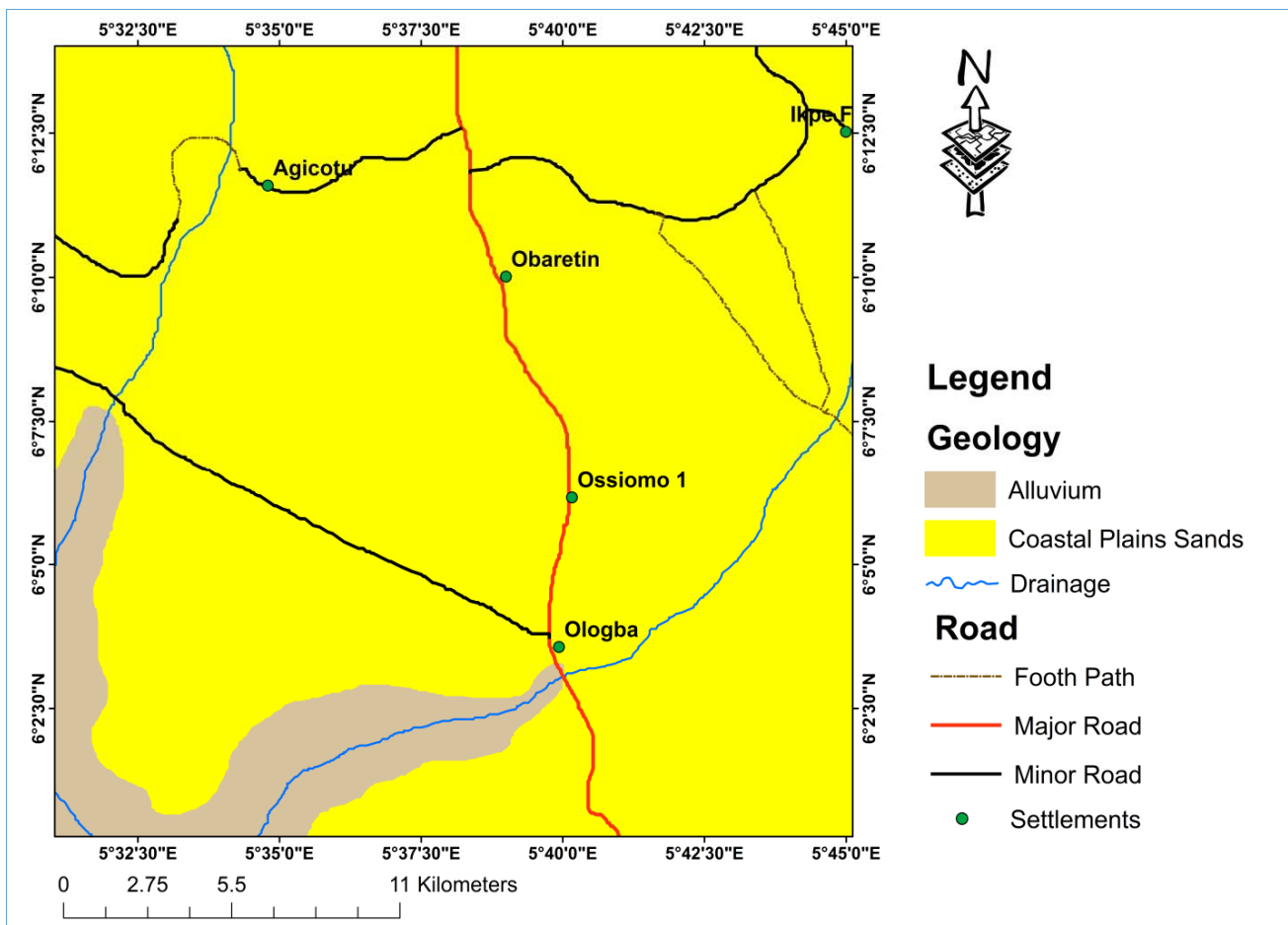


Fig. 1. Geology map of the Study Area (Obaretin)

## 4. Methodology

### 4.1. 2-D Electrical Resistivity Tomography (ERT)

In this study, ten (10) 2D resistivity traverses were acquired in a 200 x 200 m<sup>2</sup> grid using the conventional Wenner Electrode Configuration. Measurements were made at sequences of electrodes at 10, 20, 30, 40, 50 and 60 m interval using four (4) electrodes spaced at 10 m apart with inter-traverse spacing of 50 m from each other with a maximum length of 200 m each (Fig. 2).

### 4.2. 3-D Electrical Resistivity Tomography (ERT)

To obtain a better data coverage and complete subsurface information in the study area, a 3-D resistivity interpretation

model which gives the most accurate results (Loke, 2000; Eze et al., 2021) was carried out using the orthogonal set of acquired 2-D apparent resistivity data (10 traverses). This was in a view to simulate a 3D resistivity dataset for 3D inversion, which is more effective and resolute than 2D inversion especially in complex heterogenous subsurface media (Eze et al., 2021).

### 4.3. Geophysical Data Processing and Inversion

For 2-D inversion, the measured 2-D apparent resistivity data was processed and inverted to generate 2-D resistivity-depth structures that match the true subsurface resistivity images using the Earth Imager 2D software for the inversion. The

field data pseudo section and the 2D resistivity structure were produced after running the inversion of the raw data to filter out noise.

To carry out 3-D resistivity inversion, the entire orthogonal set of 2-D traverses (i.e. Y-direction and X direction) were collated to form a single 3-D data set that can be read by a default 3-D inversion program (Loke and Barker 1996;

Ahzegebobor et al. 2010; Eze et al., 2021; Eze et al., 2022) using the RES2DINV collation program code. The 3-D apparent resistivity data set was inverted using RES3DINV and Voxler 4.0 software's. The inverted files in Diprowin format were collated into a single 3D data set using a batch file and developed to obtained depth slice for each location and the 3D block visualisation of electrical resistivity tomography imaging for Obaretin.

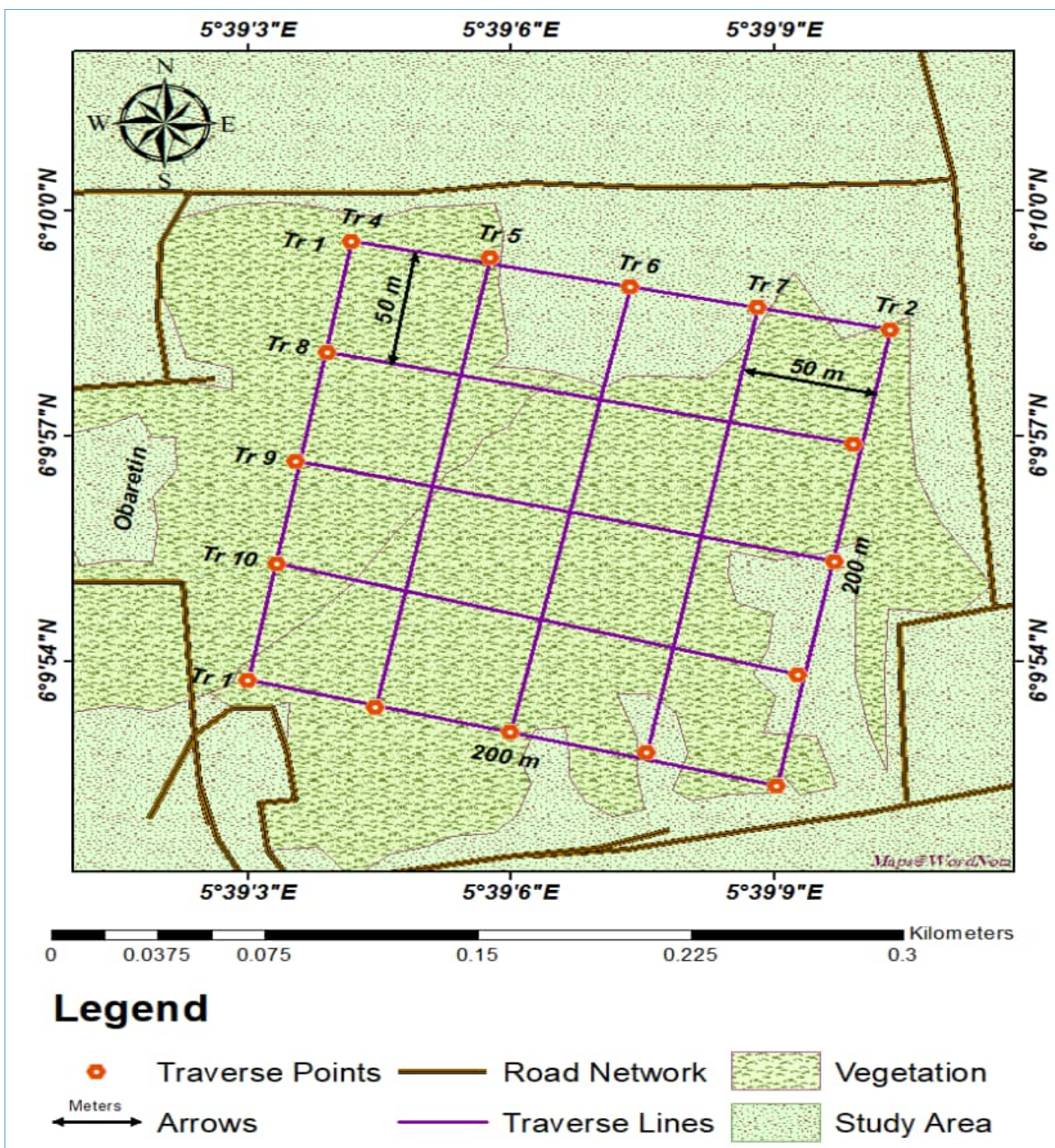


Fig. 2. Data Acquisition Map showing traverse lines in Obaretin

The volume of each of the lithologic unit was estimated using the mathematical modelling formulae for volumetric calculation shown in Equation 1. From the 3D horizontal depth slide, the area ( $\Delta A$ ) of the identified geologic formation was multiplied by the corresponding depth ( $\Delta Z$ ). The product is expressed as volume of the geologic formation ( $\Delta V$ ) (Fig. 3).

**5. Result and Discussion**

The results of 2D ERI profiles are displayed in resistivity-depth sections using Earth Imager 2D software (Figs. 4a-j). The ten 2D electrical resistivity profiling depict the various geologic formation components present in the study area. They are primarily four lithologic units namely clay/Shale deposit, clayey sand/sand, sandstone/lateritic sand and

granite deposit. For precise and effective delineation of the geologic formations in the study area, several literature reviews were consulted as guides (Alile et al., 2012; Ezomo et al., 2015; Osisanya et al., 2017; Osisanya et al., 2020; Airen and Ekhoragbon 2021; Nordiana et al., 2013). It could be deduced that clay/shale deposit in the study area has a resistivity value ranging from 1-100 Ωm, clayey sand/sand deposit has its resistivity values ranging from 100–1000 Ωm, sandstone/laterite deposit ranges from 1000–4000 Ωm, while granite deposit ranges from 5000–1,000,000 Ωm. Very low resistivity value depicts clay/shale deposit while a very high resistivity value connotes granites deposit present at the location. (Fig. 4a-j).

**5.1. Clay/Shale Deposit**

From the 2D resistivity imaging results, there is likelihood of clay/shale (deep blue coloration) in traverse 5 at a vertical depth of 30 m below to undetermined depth and at a lateral extent of 30 m to 180 m. Its resistivity value ranges from 1–100 Ωm and is sparsely deposited in the study area but not in commercial quantity. This is in line with the result of the

investigation conducted by Osisanya et al. (2020) at the study location. Owing to the vast importance of clay to the nation and the society at large, this study is of paramount importance.

**5.2. Clayey Sand/Sand Deposit**

The result of the 2D resistivity imaging obtained revealed that clayey sand/sand deposit exists in appreciable quantity virtually in all ten traverses and both sparsely and discrete deposited. Its resistivity values range from 100–1000Ωm and it could be depicted to exist virtually in all the traverses (namely 1–10) which varies from blue to green coloration. More so, it could be observed in large quantities in traverses 3, 4, 5, 6, 7, 8, 9 and 10. Alile et al. (2011) observed that the study area is a sedimentary basin which consists 90% intercalation of sandstone and clay. Similarly, Alsulaimani et al. (2016) conducted an investigation to quantify the silica sand deposit in Saudi Arabia by using core control and geophysical approach. It was discovered from the results of both methods adopted that the volume of sand deposit in the area was in large quantity.

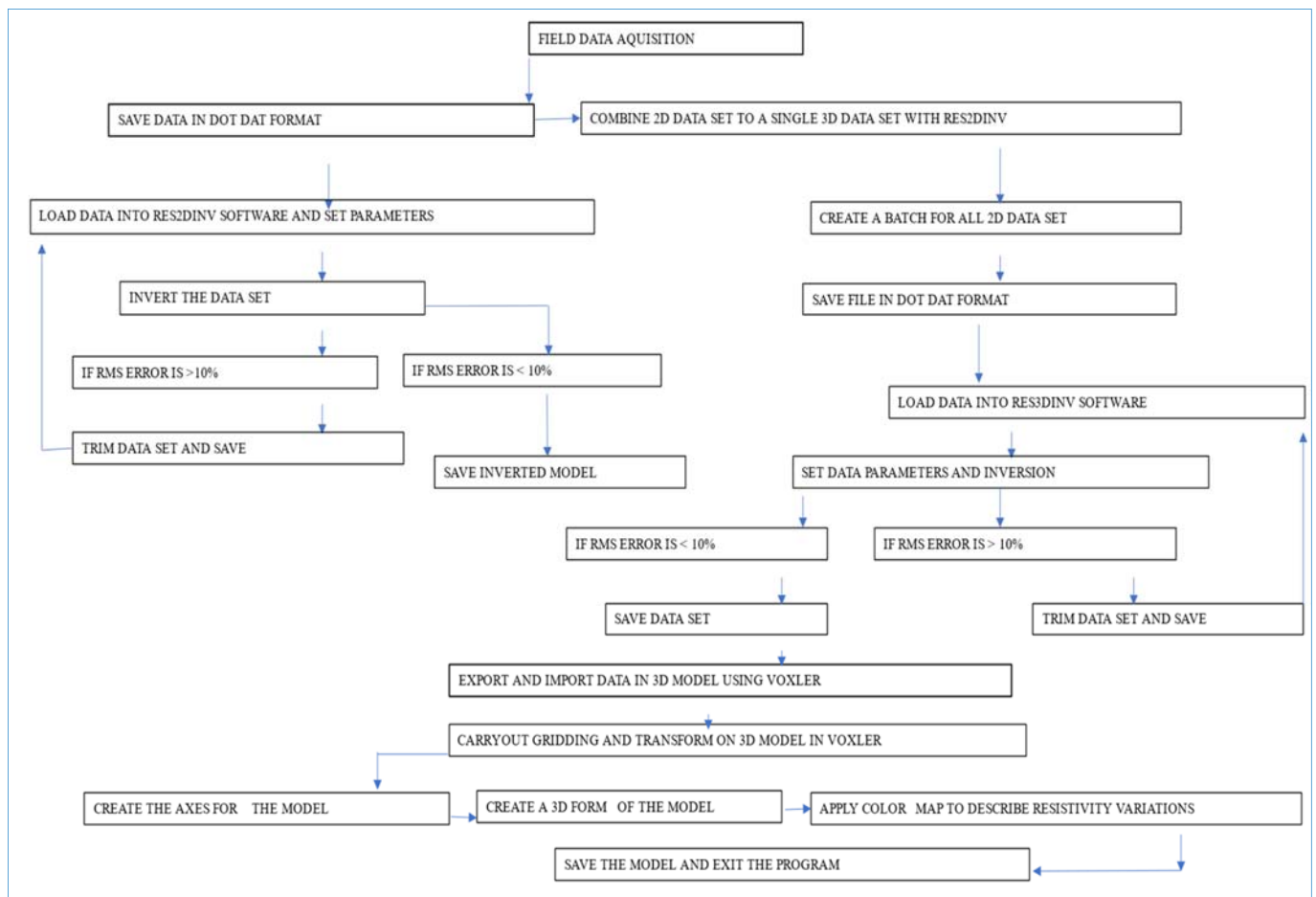


Fig. 3. Flowchart showing workflow procedures employed in the study

**5.3. Sandstone/Lateritic Sand Deposit**

This could be seen to exist in quite appreciable quantities in virtually all the traverses. Although, it is sparsely and massively deposited at different depths. Its resistivity values range from 1000-4000Ωm and could be deduced to be one of

the dominant formations in the study area which is fairly commercially exploitable. From the results of the ten horizontal profiling conducted, laterite (blue to green coloration) deposit could be seen to exist in relatively large quantity in all the profiles namely traverses (1–10) and are

found to be commercially exploitable. This is in line with the result of the investigation conducted by [Osisanya et al. \(2017\)](#) at the study area.

Table 1. Resistivity values of common rocks and soil materials ([Keller and Frischknecht, 1996](#); [Nordiana et al., 2013](#))

Material	Resistivity ( $\Omega$ -m)
Alluvium	10 to 800
Sand	60 to 1000
Clay	1 to 100
Groundwater (fresh)	10 to 100
Sandstone	$8 - 4 \times 10^3$
Shale	$20 - 2 \times 10^3$
Limestone	$50 - 4 \times 10^3$
Granite	5000 to 1,000,000

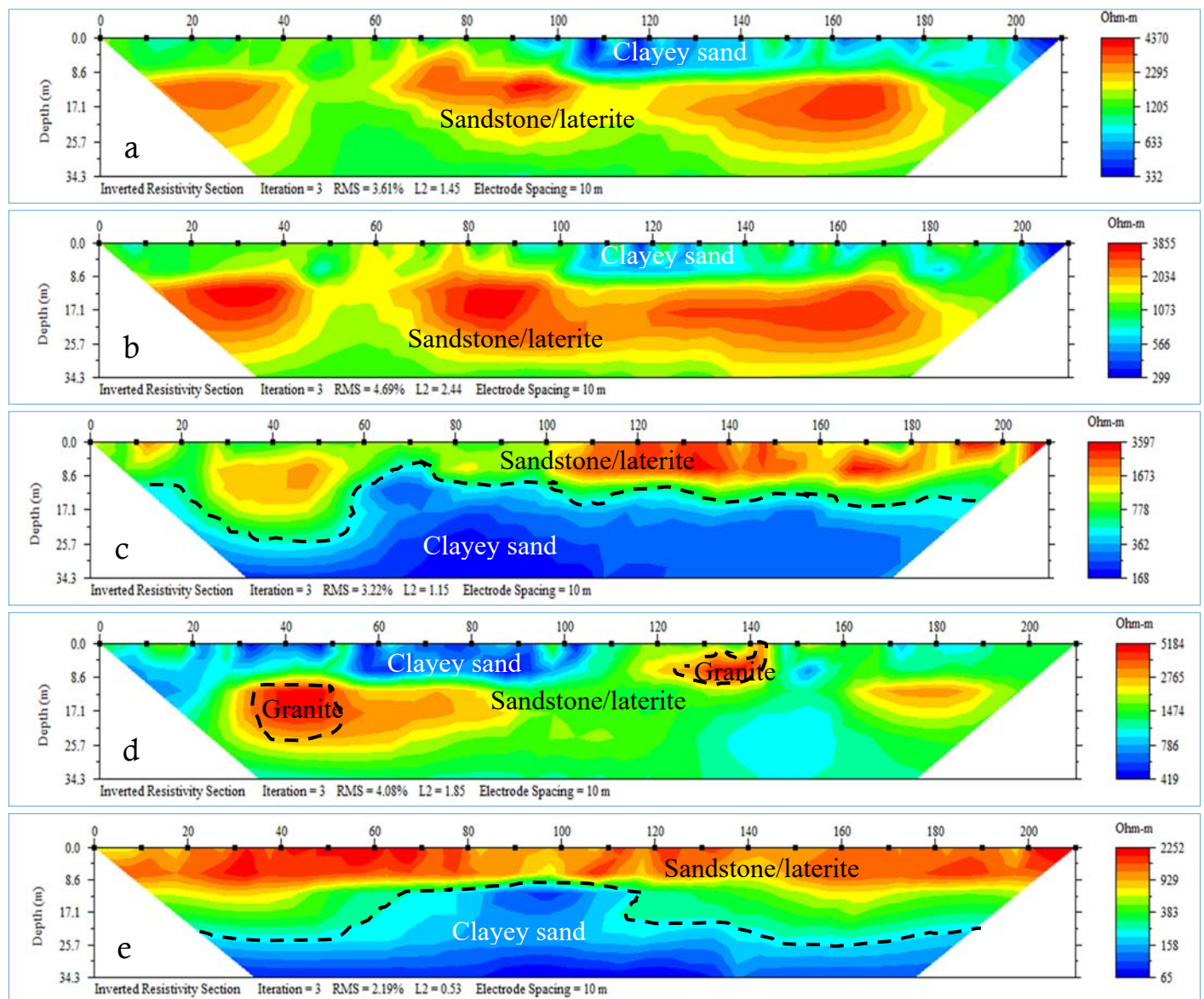
**5.4. Granite Deposit**

Granite deposit is depicted with very high resistivity values which are 5000  $\Omega$ m to 1,000,000 from the horizontal profiling. The resistivity values of transverse 4 and 6 depict

the probable presence of granite deposit while all other transverses reveal no presence of the formation ([Table 1](#)). [Nordiana et al. \(2013\)](#) stated that structural and stratigraphic features of granite deposit can be delineated effectively with the use of 2-D resistivity tomography along side with Enhancing Horizontal Resolution.

In [Fig. 5](#), horizontal depth slices are used to represent the 3D inverse model of the smoothness restricted least square inversion that was created from the data set of the 2D inverse model. The inversion of the 3D collated data set were produced according to [White et al. \(2001\)](#) and [Li and Oldenburg \(1994\)](#).

A RMS error of 6.37% was observed and the number of model level is five. The electrical resistivity value for the models are ranging from 49.8–3253  $\Omega$ m for unit electrode spacing of 10.0 m. The estimated model for the five different depth slice is at depth interval of about 1m while the first, second, third, fourth and fifth layers have thicknesses of 5 m, 5.8 m, 6.6 m, 7.6 m and 8.7 m respectively.



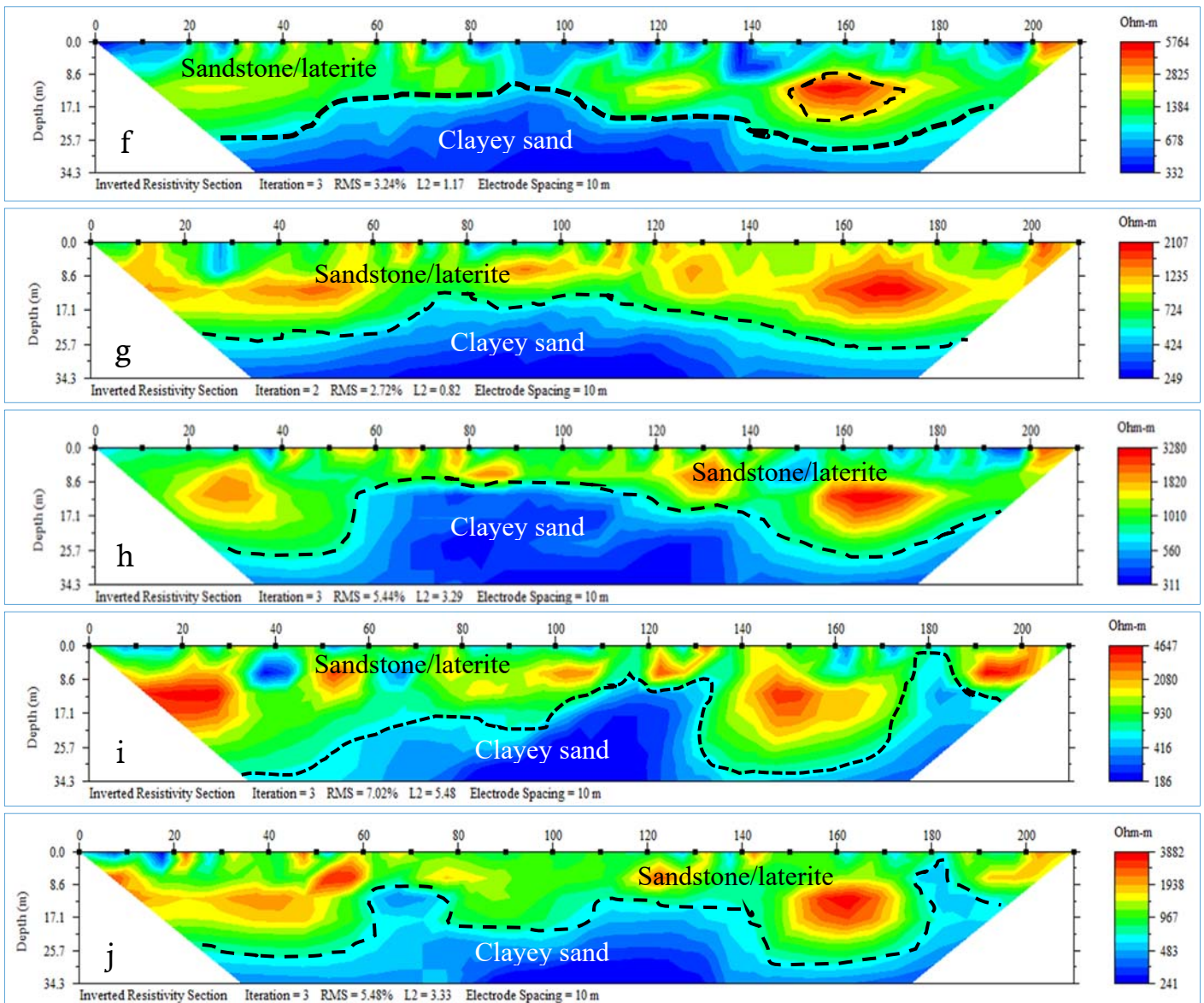


Fig. 4. 2D electrical resistivity-inverted sections showing different geologic formations: a) 2D Resistivity-depth structure for Traverse 1, b) 2D Resistivity-depth structure for Traverse 2, c) 2D Resistivity-depth structure for Traverse 3, d) 2D Resistivity-depth structure for Traverse 4, e) 2D Resistivity-depth structure for Traverse 5, f) 2D Resistivity-depth structure for Traverse 6, g) 2D Resistivity-depth structure for Traverse 7, h) 2D Resistivity-depth structure for Traverse 8, i) 2D Resistivity-depth structure for Traverse 9, and j) 2D Resistivity-depth structure for Traverse 10

The 2D horizontal slice (Fig. 5) depicts that these five model layers are composed of intercalation of sand and clay, large volume of gravel surrounded with laterite, intercalation of sand and clay, large volume of clayey sand surrounded with laterite and large volume of clay enclosed by laterite respectively. Laterite deposit was found to be massively deposited and commercially exploitable while clay deposit was found to be sparsely deposited and not in very large volume. The vertical slice has x and y unit electrode spacing of 10m with a RMS of 5.20%.

The Obaretin study area's 3D model is seen in Figure 6. The depth imaged was 29 m below the subsurface. The model demonstrated that, with the exception of the anterior view, where the resistivity value increases from 3.207 m to 3.417 m, this research area is reasonably uniform, with a resistivity value of about 3.628 m in logarithmic value. This resistivity value is indicative of clay (1.73–2.336 Ωm), clayey sand

(2.36–2.785 Ωm), silt sand (2.996–3.207 Ωm), lateritic sand with sandstones (3.207–3.417 Ωm) and gravel deposit (3.517 Ωm).

The result of the 3D resistivity image is in line with the 2D x and y horizontal and vertical slices obtained because it revealed a large deposit of laterite and sand formations with sparse deposit of intercalation of sand and clay geologic formation.

**5.5. Correlation of Borehole Lithology in Obaretin**

Fig. 7 below show the lithological logs obtained at Obaretin. The boreholes were drilled to a depth of about 40 m each. The logs show that the subsurface at this location is composed of sand and clayey sand materials though with varying grain sizes and compactness.

The first substratum that could be called the topsoil is a

clayey sand material that extends from the surface to about 5 m. This is underlain by a coarse dry sand material that extends from a depth of about 5 m to as deep as 19 m. Underlying the coarse dry sand is a medium-coarse sand

material occurring at a depth range of 19–38 m. The last horizon obtained at the two boreholes is a clayey sand the thickness of this stratum could not be ascertained (Table 2).

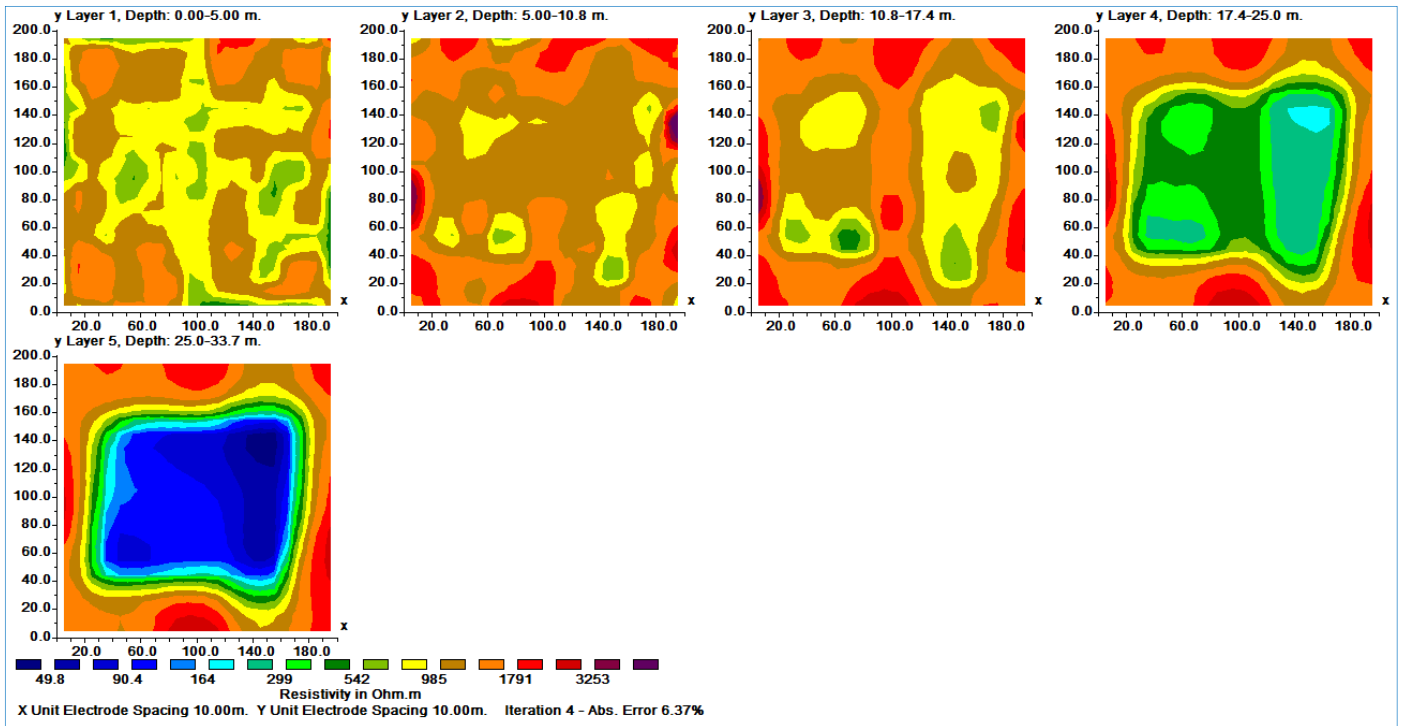


Fig. 5. Five-layer horizontal depth slices obtained from 3D inversion of orthogonal 2D profiles using smoothness constrained least square inversion

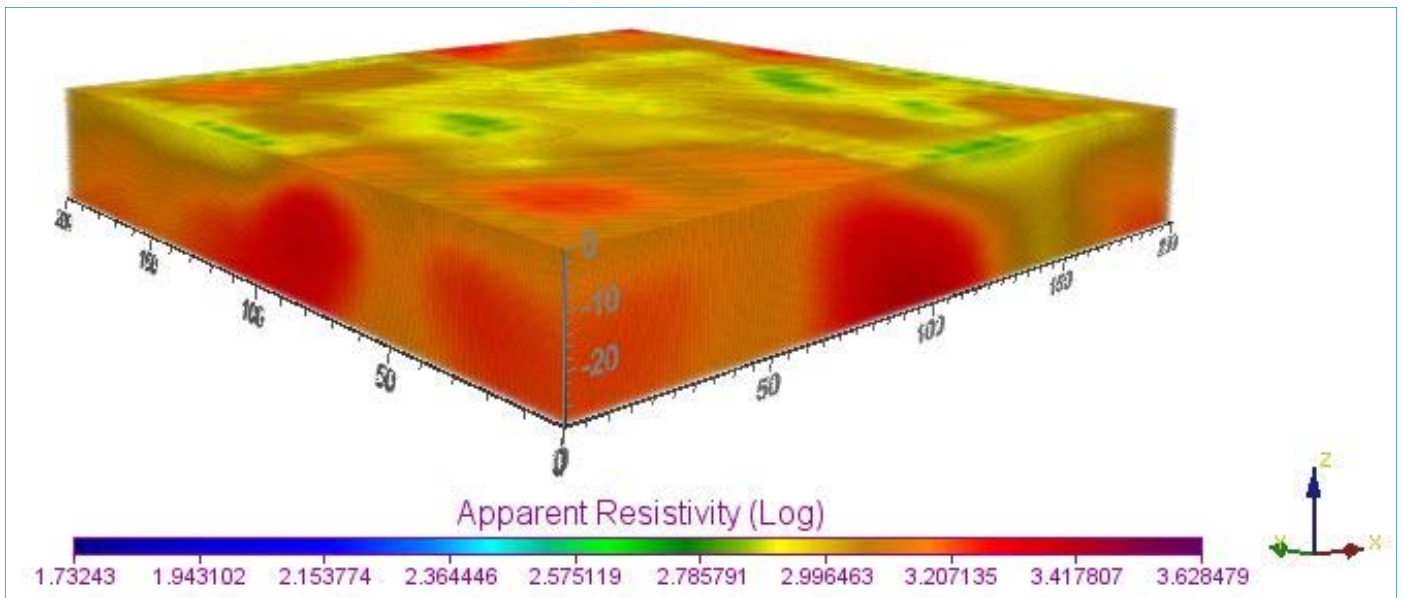


Fig. 6. 3D Electrical Resistivity Tomography Volume beneath study area (along Obaretin)

Table 2. Resistivity lithology of survey in Obaretin

Depth (m) (in range)	Resistivity ( $\Omega$ m) (in range)	Geologic formation
0 – 5	299 – 1791	Silt sand top
5 – 20	985 – 3253	Lateritic sand with sandstones intercalations
20 – 40	49.8 – 1791	Clayey sand

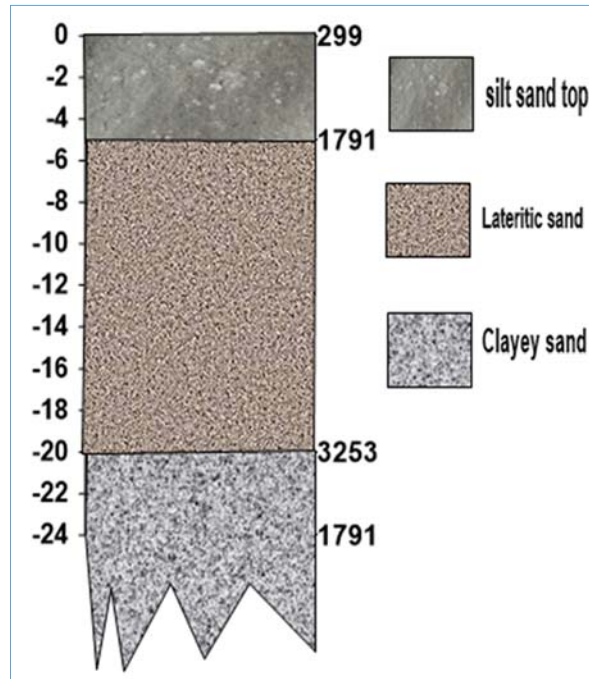


Fig. 7. Resistivity lithology of the study area at Obaretin

Table 3. Approximated estimate of volume of silt sand soil in Obaretin

Layers	Layers depth (in range)	Area $\Delta A$ (m <sup>2</sup> )	Depth $\Delta Z$ (m)	Volume $\Delta V$ (m <sup>3</sup> )
1	0 – 5	15900	5.0	79,500
2	5 – 10.8	14700	5.8	85,260
3	10.8 – 17.4	18600	6.6	122,760
4	17.4 – 25	11400	7.6	86,640
5	25 – 33.7	16800	8.7	146,160
Total				520,320

Table 4. Approximated estimate of volume of clayey sand in Obaretin

Layers	Layers depth (in range)	Area $\Delta A$ (m <sup>2</sup> )	Depth $\Delta Z$ (m)	Volume $\Delta V$ (m <sup>3</sup> )
1	0 – 5	0	5.0	0
2	5 – 10.8	0	5.8	0
3	10.8 – 17.4	0	6.6	0
4	17.4 – 25	6400	7.6	48,640
5	25 – 33.7	16800	8.7	146,160
Total				194,800

Table 5. Approximated estimate of volume of lateritic sand in Obare in Obaretin

Layers	Layers depth (in range)	Area $\Delta A$ (m <sup>2</sup> )	Depth $\Delta Z$ (m)	Volume $\Delta V$ (m <sup>3</sup> )
1	0 – 5	9400	5.0	47,000
2	5 – 10.8	6700	5.8	38,860
3	10.8 – 17.4	6880	6.6	45,408
4	17.4 – 25	13100	7.6	99,560
5	25 – 33.7	16400	8.7	142,680
Total				373,508

Table 6. Summary of approximate percentage estimate of volume of suspected dominant

Sample No	Lithologic units (sand)	Volume (m <sup>3</sup> )	Percentage (%)
1	Lateritic	373,508	34.00
2	Silt sand	520,320	47.79
3	Clayey sand	194,800	17.89
Total		1,088,628	100

Obaretin study area showed three geoelectric subsurface which includes silty sand topsoil (299–1791  $\Omega\text{m}$ ), lateritic sand with sandstones intercalations (985–3253  $\Omega\text{m}$ ), and clayey sand (48.9–1791  $\Omega\text{m}$ ). This lithology corroborates with the lithology of borehole log within the environs.

### 5.6. Volumetric Analysis of the Dominant Geologic Formations

In Obaretin, sand and laterite deposits are thought to be the main subsurface components. An estimation of the area of zones measured through x-y axes from the 3D horizontal slices is made using a visual observation to determine the volume of the suspected dominant geologic formation. The volume of Sand was calculated using a straightforward mathematical modeling method. The corresponding depth (Z) was multiplied by the estimated identified sand area (A) from a 3D horizontal slice.

The product is expressed as volume ( $\Delta V$ ) for the associated sand in a layer,  $\Delta V = \Delta A \times \Delta Z$  (Abdullahi et al., 2013). The approximate estimate of volume of dominant geologic formation. in Obaretin is shown in Table 3 to Table 5. Table 6 shows the summary of approximate percentage estimate of volume of dominant geologic formations in Obaretin.

### 6. Conclusion

In Obaretin, the 2D resistivity values ranges between 73.4 – 3838  $\Omega\text{m}$  at a depth range of 2.5–39.6 m. The 3D resistivity values ranges between 49.8–3253  $\Omega\text{m}$  at a depth range of 0–33.7 m. The Resistivity lithology of the study areas showed three geo-electric subsurface to appreciable depth of 40 m; Silty sand topsoil (299–1791  $\Omega\text{m}$ ), lateritic sand with sandstones intercalations (985–3253  $\Omega\text{m}$ ), and clayey sand (48.9–1791  $\Omega\text{m}$ ). The lithology corroborates with borehole log within the environs. The study revealed that the dominant formations are laterite, silty sand and clayey sand which have estimated volume of 373,508  $\text{m}^3$ , 520,320  $\text{m}^3$  and 194,800  $\text{m}^3$  per two million  $\text{m}^3$ . Hence, the adoption of 2D and 3D electrical resistivity imaging has aided the successful volumetric assessment of geologic formation in the study area.

### Conflict of Interest

On behalf of all authors, the corresponding author declares that there is no conflict of interest. Potential conflicts do not exist regarding the work.

### Data availability statement

My manuscript has associated data in a data repository.

### References

- Abdelwahab, H., 2013. Comparison of 2D and 3D Resistivity Imaging Methods in the Study of Shallow Subsurface Structures. *Greener Journal of Physical Sciences* 3 (4), 149-158.
- Abdullahi, A., Mohd, N.M.N., Rosli, S., Kola, A.N.A., 2013. Volumetric Assessment of Leachate from Solid Waste using 2D and 3D Electrical Resistivity Imaging, *Advanced Materials Research* 726-731 (2013), 3014-3022.
- Abolarin, O.M., Eze, U.S., Ibitoye, T.A., Bello, A.M., Nnorom, S.L., 2020. Multitechnique Mineral Exploration in A Part of Igarra North Basement Complex of Southwestern Nigeria. *Geosciences* 10 (1), 10-24.
- Ahzebobor, P.A., Olayinka, A.I., Singh, V.S., 2010. Application of 2D and 3D geoelectrical resistivity imaging for Engineering site investigation in a crystalline basement terrain, Southwestern Nigeria. *Environmental Earth Sciences* 61 (7), 1481-1492. <https://doi.org/10.1007/s12665-010-0464-z>.
- Airen, O.J., Ekhorgbon, M.O., 2021. The Use of Electrical Resistivity Tomography to Classify the Earth's Subsurface in Ugbogiobo Community, Edo State, South-South Nigeria. *Nigerian Journal of Technology* 40 (5), 966 -975.
- Alile, O.M., Aigbogun, C.O., Enoma, N., Abraham, E.M., Ighodalo, J.E., 2017. 2D and 3D Electrical Resistivity Tomography (ERT) Investigation of Mineral Deposits in Amahor, Edo State, Nigeria. *Nigerian Research Journal of Engineering and Environmental Sciences* 2 (1) 215-231.
- Alile, O.M., Ujuanbi, O., Evbuomwan, I.A., 2011. Geoelectric investigation of groundwater in Obaretin – Iyanomon locality, Edo state, Nigeria. *Journal of Geology and Mining Research* 3 (1), 13-20.
- Alile, O.M., Abraham, E.M., 2015. Three-dimensional geoelectrical imaging of the subsurface structure of university of Benin-Edo state Nigeria. *Advances in Applied Science Research* 6 (11), 85-93.
- Alsulaimani, G., Ahmed, M.F., Raza, M., 2016. Reserve Estimation of Silica Sand Deposits by Core Control and Geophysical Methods, A Case Study from Saudi Arabia. *The Nucleus* 53 (3), 162-170.
- Bermejo, L., Ortega, A.I., Guérin R., Benito-Calvo, A., Perez-Gonzalez, A., Peres, J.M., Aracil, E., de Casto, J.M.B., Carbonell, E., 2017. 2D and 3D ERT imaging for identifying karst morphologies in the archaeological sites of Gran Dolina and Galería Complex (Sierra de Atapuerca, Burgos, Spain). *Quaternary International* 433, 393-401. <https://doi.org/10.1016/j.quaint.2015.12.031>.
- Bery, A.A., Saad, R., Mohamad, E.T., Jinmin, M., Azwin, I.N., Tan, N.M.A., Nordiana, M.M., 2012. Electrical resistivity and induced polarization data correlation with conductivity for iron ore exploration. *The Electronic Journal of Geotechnical Engineering* 17, 3223-3233.
- Bhattacharya, B.B., Shalivahan, S., 2016. *Geoelectric methods: theory and applications*: McGraw Hill Education (India) Private Limited.
- Cheng, Q., Chen, X., Tao, M., Binley, A., 2019. Characterization of karst structures using quasi-3D electrical resistivity Tomography. *Environmental Earth Sciences* 78 (2019), 285 <https://doi.org/10.1007/s12665-019-8284-2>.
- Dahlin, T., Zhou, B., 2006. Gradient array measurements for multi-channel 2D resistivity imaging. *Near Surface Geophysics* 4, 113-123.
- Eze, S.U., Ogagarue D.O., Nnorom, S.L., Osung, W.E., Ibitoye, T.A., 2021. Integrated geophysical and geochemical methods for environmental assessment of subsurface hydrocarbon contamination. *Environ Monit Assess* 451 (2021) 193-451. <https://doi.org/10.1007/s10661-021-09219-3>.
- Eze, S.U., Orji, O.M., Onoriode, A.E., Saleh, S.A., Abolarin, M. O., 2022. Integrated Geoelectrical Resistivity Method for Environmental Assessment of Landfill Leachate Pollution and Aquifer Vulnerability Studies. *Journal of Geoscience and Environment Protection* 10, 1-26. <https://doi.org/10.4236/gep.2022.109001>.
- Ezomo, F.O., Justice, E.A., Ojeabu, A., Ezekiel, A., 2015. Delineation of Subsurface Lithology using Two-Dimensional Geoelectrical Resistivity Imaging in Ologbo Area of Edo State, Nigeria. *International Journal of Scientific & Engineering Research* 6, June-2015.

- Keshavarzi, M., Baker, A., Kelly, B.F., Andersen, M.S., 2017. River-groundwater connectivity in a karst system, Wellington, New South Wales, Australia. *Hydrogeology Journal* 25 (2), 557-574.
- Keller, G.V., Frischknecht F.C., 1996. *Electrical methods in geophysical prospecting*. Pergamon Press Inc., Oxford, United Kingdom.
- Khalil, M.A., Santos, F.M., Cach, M., Fonseca, P.E., Mata, J., 2013. 2D and 3D Resistivity Tomography of the Su'imo Garnet-bearing Byke, Lisbon Volcanic Complex, Portugal: a case study. *Journal of Geophysics and Engineering*. *Journal of Geophysics Engineering* 10, 035013.
- Kogbe, C.A., 1989. *Geology of Nigeria*. Rock View (Nig.) Ltd., Plot 1234, Zaramaganda, Km 8, Yakubu Gowon Way, Jos, Nigeria. First published 1975, pp. 39-56.
- Lesmes, D.P., Friedman, S.P., 2005. Relationships between the electrical and hydrogeological properties of rocks and soils. In: Rubin Y, Hubbard SS (eds) *Hydrogeophysics*. Springer, New York, pp 87-128.
- Li, Y., Oldenburg, D.W., 1994. Inversion of 3D DC Resistivity Data using an Approximate Inverse Mapping. *Geophysical Journal International*, 116, pp. 527-537.
- Longo, V., Testone, V., Oggiano, G., Testa, A., 2014. Prospecting for clay minerals within volcanic successions: application of electrical resistivity tomography to characterize bentonite deposits in northern Sardinia (Italy). *Journal of Applied Geophysics* 111, 21-32.
- Loke, M.H., 2000. *Electrical imaging surveys for environmental and engineering studies: a practical guide to 2-D and 3-D surveys*, 1-20.
- Loke, M.H., 2012. Tutorial: 2-D and 3-D electrical imaging surveys, 1-18.
- McCormack, T., O'Connell, Y., Daly, E., Gill, L.W., Henry, T., Perriquet, M., 2017. Characterisation of karst hydrogeology in Western Ireland using geophysical and hydraulic modelling techniques. *Journal of Hydrology: Regional Studies* 10, 1-17.
- Ogunsanwo, O., 1989. Some properties of sedimentary laterite soil as engineering construction material. *International Association of Engineering Geology Bulletin*, 39 (1), 131-135.
- Nordiana, M.M., Saad, R., Nawawic, M.N.M., Azwind, I.N., Tonnizam, M., 2013. Case Study: Shallow Subsurface Geology Mapping Using 2-D Resistivity Imaging with EHR Technique. *Sciverse sciencedirect. APCBEE Procedia* 5, 134-140.
- Osisanya, O.W., Ibitoye, A.T., Eze, S., Ezomo, F.O., Okeh, O., 2017. Delineation of Laterite Deposits using Two-Dimensional Geo-Electric Imaging in Agbonmwoba Village Area of Obaretin Town, Edo State, Nigeria. *Journal of Emerging Trends in Engineering and Applied Sciences* 8 (6), 233-243.
- Osisanya, O.W., Abolarin, O.M., Korode, A.I., Ajibade, Z.F., 2020. 2D Geo-electrical Resistivity Imaging of Clay Deposit in Agbonmwoba Village, Edo State, Nigeria. *Journal of Environment and Earth Science* 10, 10. <https://doi.org/10.7176/JEES/10-10-06>.
- Panek, T., Hradecky, J., Silhan, K., 2008. Application of electrical resistivity tomography (ERT) in the study of various types of slope deformations in anisotropic bedrock: case studies from the Flysch Carpathians. *Studia Geomorphologica Carpatho-Balcanica* 42, 57-73.
- Piegari, E., Cataudella, V., Di Maio, R., Milano, L., Nicodemi, M., Soldovieri, M.G., 2009. Electrical resistivity tomography and statistical analysis: a conceptual approach. *Journal of Applied Geophysics* 68, 151-158. <https://doi.org/10.1016/j.jappgeo.2008.10.014>.
- Revil, A., Leroy, P., Titov, K., 2005. Characterization of transport properties of argillaceous sediments. Application to the Callovo-Oxfordian Argillite. *Journal of Geophysical Research* 110, B06202.
- Robert, T., Dassargues, A., Brouyère, S., Kaufmann, O., Hallet, V., Nguyen, F., 2011. Assessing the contribution of electrical resistivity tomography (ERT) and self-potential (SP) methods for a water well drilling program in fractured/karstified limestones. *Journal of Applied Geophysics* 75 (1), 42-53.
- Savin, C., Robineau, B., Monteil, G., Beauvais, A., Parisot, J.C., Ritz, M., 2003. Electrical imaging of peridotite weathering mantles as a complementary tool for nickel ore exploration in New Caledonia: ASEG 16th Geophysical Conference and Exhibition, Extended Abstracts, 1-5.
- Schrott, L., Saas, O., 2008. Application of field geophysics in geomorphology: advances and limitations exemplified by case studies. *Geomorphology* 93, 55-73.
- Xu, S., Sirieix, C., Marache, A., Riss, J., Malaurent, P., 2016. 3D geostatistical modeling of Lascaux hill from ERT data. *Engineering Geology* 21, 169-178.
- White, R.M.S., Collins, S., Denne, R., Hee, R., Brown, P., 2001. A new survey design for 3D IP modelling at sCopper Hill. *Exploration Geophysics* 32, 152-155.